

Whole-rock geochemistry of Tertiary sediments of Mizoram Foreland Basin, NE India: implications for source composition, tectonic setting and sedimentary processes

M. Faruque Hussain¹ · Bubul Bharali²

Received: 16 August 2018 / Revised: 24 October 2018 / Accepted: 7 January 2019 / Published online: 14 January 2019
© Science Press and Institute of Geochemistry, CAS and Springer-Verlag GmbH Germany, part of Springer Nature 2019

Abstract Sandstones belonging to the Oligocene Barail Group and Miocene Surma Group of the Mizoram Foreland Basin have been studied geochemically to constrain their provenances, tectonic setting, and other sedimentary processes (weathering and mineral sorting etc.). Based on their mineralogical compositions, these sandstones are classified as quartzarenite and sublithic-arenite. The sandstones of Barail and Surma Groups have similar contents of most of the major elements except for SiO_2 and Al_2O_3 . The Barail sandstones are relatively more siliceous and less aluminous compared to the Surma sandstones. Barail and Surma sandstones were plotted in a singular array on different geochemical discrimination diagrams. The CIA and CIW values of the sandstones of Barail (69 and 77 respectively) and Surma Groups (68 and 77 respectively) suggest that the sandstones were derived from moderately weathered source rocks. In the A–CN–K diagram, the studied samples plotted along a roughly singular trend that originates from granodiorite as well as Trans-Himalayan granitoids and also confined within the field of Siwalik sediments. Chondrite-normalized REE patterns for the Surma and Barail sandstones are identical and are similar to upper continental crust, with moderate to high LREE enrichment and prominent negative Eu anomalies (Eu/Eu^* for both Barail and Surma sandstone = 0.69), indicating their derivation from a felsic magmatic source. The values of Eu/Eu^* , $(\text{La}_N/\text{Lu}_N)$, La/Sc , La/Co , Th/Sc , Th/Co , and $\text{Cr}/$

Th ratios of Surma and Barail sandstones are also not significantly different, and the values are similar to fine-fractions derived from the weathering of felsic rocks. In the $\text{K}_2\text{O}/\text{Na}_2\text{O}$ versus SiO_2 , Th–Sc–Zr/10 and Ti/Zr versus La/Sc tectonic discrimination diagrams the studied samples of Barail and Surma sandstones plot within the fields of greywacke from continental island arcs and active continental margin. The geochemical characteristics of the studied sedimentary rocks and their similarity with the Siwalik foreland sediments thus suggest were sourced from different felsic magmatic lithounits of Himalaya and were deposited in an active continental margin.

Keywords Geochemistry · Sandstone · Barail and Surma Groups · Mizoram Foreland Basin · Northeast India

1 Introduction

Synorogenic clastic sedimentary rocks of foreland basins are important for understanding their composition, tectonic history, and provenance with an implication to the origin and evolution of the orogen(s). Geochemical characteristics of clastic sedimentary rocks provides clues to decipher provenance (Floyd et al. 1989; Feng and Kerrich 1990; Condie 1993; McLennan et al. 1993; Hayashi et al. 1997; Cullers and Podkorytov 2002; Bracciali et al. 2007; Wang et al. 2012), tectonic setting (Bhatia 1983; Bhatia and Crook 1986; Roser and Korsch 1986; Wang et al. 2012), weathering indices, and paleoclimatic conditions (Parker 1970; Nesbitt and Young 1982; Cox et al. 1995; Fedo et al. 1995; Clift et al. 2008; Yin et al. 2010). The Mizoram Foreland Basin (MFB) in the northeastern part of India is surrounded by Eastern Himalayan Ranges, Naga Hill Ranges, and Mikir Hills Massif in the north; Shillong

✉ M. Faruque Hussain
faruque_geo@yahoo.co.in

¹ Department of Earth Science, Assam University, Silchar, Assam 788 011, India

² Department of Geology, Pachhunga University College, Aizawl, Mizoram 796 005, India

Plateau in the northwest, and Indo-Burman Ranges in the east-southeast direction. The basin is filled with sediments represented by Barail, Surma, and Tipam Groups derived from Himalaya and other surrounding orogens. MFB can be considered as a sub-basin of Bengal basin. The Bengal basin encompasses the entirety of Bangladesh and some parts of NE India including Assam, Mizoram, Manipur, and Tripura. The Bengal basin in Bangladesh is divided into three geological provinces: (1) Northwestern shelf (NWS, Province 1); (2) Northeastern, or Surma basin (Province 2); and (3) Southeastern, or Chittagong-Tripura Folded Belt (CTFB, Province 3) (Reimann 1993; Uddin and Lundberg 1998; Najman 2006; Najman et al. 2008). MFB constitutes the eastern extension of CTFB within Indian Territory. The sedimentary sequences belonging to Barail and Surma Groups from different geological provinces of Bengal basin were studied by several workers and suggested sourced chiefly from different Eastern Himalayan felsic lithounits (see e.g. Uddin and Lundberg 1998; Rahman and Suzuki 2007; Najman et al. 2008; Hossain et al. 2010; Rahman et al. 2014, 2017). The sediments of MFB however are very scantily studied and more particularly in terms of their geochemical characteristics, due to their difficult terrain condition and remote location. A recent study, made by Sawant et al. (2017), with samples collected mainly from the Surma Group of Mizoram basin have suggested that these sediments were derived from the Precambrian cratonic crust of Shillong plateau. In the present paper, we provide the results of the geochemical study of the sandstones from the Oligocene Barail Group and Miocene Surma Group of MFB to understand the provenance, tectonic setting and sedimentary differentiation processes (weathering and hydraulic sorting) for the sediments.

2 Geological setting

The Mizoram Foreland Basin covers an area of about 21,087 km² within 21°56'N to 24°31'N, and 92°16'E to 93°26'E. The geology and distribution of sediments in the MFB are presented in Fig. 1a. The stratigraphic succession with lithology and thickness (after Karunakaran 1974) are presented in Fig. 1b. MFB is comprised predominantly of folded Tertiary clastic sedimentary rocks belonging to the Surma and Barail Groups with a fold axis oriented along the N–S direction. The folding in the sediments of MFB is normally wider in the central part compared to the southern part and the intensity of folding increases towards the margin orogen (Dasgupta 1984). The Oligocene Barail Group, Miocene Surma Group, and Pliocene Tipam Group of sediments comprise the Tertiary succession of the MFB from bottom upwards (Fig. 1b). The Tipam Group of rocks

were restricted in a narrow strip in the north-western part of the basin, while the Barail Group of rocks occur towards the eastern part of the basin bordering Myanmar (Fig. 1a). The rest of the basin is occupied predominantly by the Surma Group of rocks (Fig. 1a). The Surma Group is divided into Bhuban and Bokabil Formations (Mathur and Evans 1964; Nandy 2001). The Bhuban Formation is the thickest developed lithostratigraphic unit in MFB with a thickness of about 5000 m, which is divided into Lower, Middle, and Upper Bhuban units (Dasgupta 1984; Nandy 2001; Tiwari et al. 2006) based on the lithologic characteristics and fossil content. The entire sediment column of the Bhuban Formation is a repetitive succession of arenaceous and argillaceous layers. The Lower Bhuban Formation is comprised of alternating shale and sandstone layers. The Middle Bhuban Formation, which represents nearly 50% of the total depository of Surma Group, is comprised predominantly of argillaceous sequences with subordinate sandstones. The Upper Bhuban Formation consists of alternating arenaceous and argillaceous layers of roughly equal thickness. The rock types of the Surma Group are sandstone, siltstone, shale, mudstone, and their mixtures in various proportions. Sandstones are generally grey colored, fine to medium grained, and often associated with shale clasts.

Sediments of the Barail Group were deposited under marine conditions, while those of the Surma Group are thought to be deposited in shallow marine to transitional conditions (Tiwari and Mehrotra 2002; Ralte et al. 2011). The sediments of Tipam Group were deposited in estuarine/fluvial environments (Sinha and Sastri 1973; Karunakaran and Ranga Rao 1979). Based on magnetostratigraphic studies Malsawma et al. (2010) have suggested the Bhuban Formation was deposited between 12.5 and 8 Ma with a significant increase in the rate of sedimentation at ~ ca.9.5 Ma.

3 Materials and methods

Thirty fresh sandstone samples (Surma Group = 20; and Barail Group = 10) were collected for the present study from outcrops around Aizawl district of Mizoram and along the road cuts on the National Highway NH-102B (Aizawl-Champhai; Fig. 1a). Twenty-five thin-sections were prepared following standard techniques, and petrographic studies were carried out. After the petrographic screening for minimal alteration, eighteen least altered sandstone samples (10 samples of Surma Group and 8 samples of Barail Group) were selected for geochemical studies. The rock samples selected for geochemical analysis were reduced to a smaller size (~ 2 cm) to observe any traces of fossils. The chips were further crushed to yet smaller sizes (~ 2 mm), then

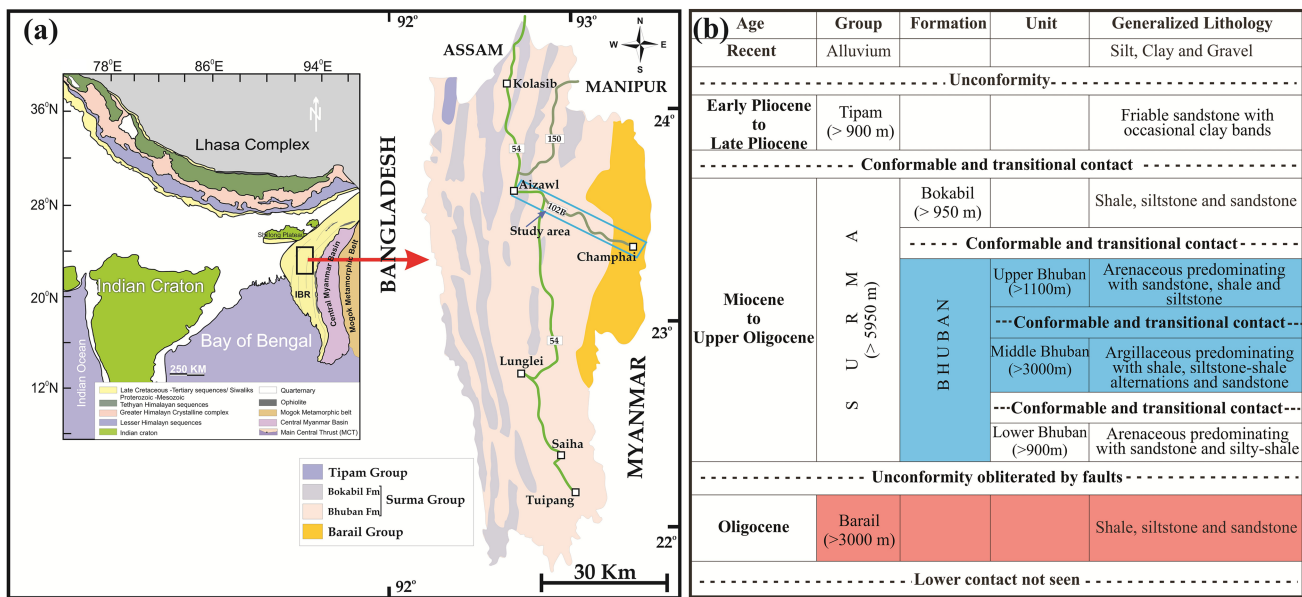


Fig. 1 **a** Geological map of the Mizoram Foreland Basin (MFB), Northeast India (after GSI 1974), along with a simplified map of India showing the distribution of Indian craton and the geological and tectonic units of Himalayan orogen and the rough location of MFB marked as a box (modified after O'Brien 2001; Mitchell et al. 2007; Webb et al. 2011) and **b** stratigraphic succession of the Mizoram Basin along with lithology and thickness (compiled from Karunakaran 1974; Tiwari et al. 2006). The study area is shown as a rectangular box in the Geological map of MFB

washed with distilled water and sundried. These samples were then pulverized using an agate mortar at Wadia Institute of Himalayan Geology (WIHG), Dehradun, India. Major oxides were determined by X-ray Fluorescence Spectrometer (XRF) on a Siemens SRS-3000 instrument, using pressed pellet following procedures described in Saini et al. (2000). Trace elements including rare earth elements were analyzed by Inductively Coupled Plasma Mass Spectrometry (ICP-MS) (ELAN-DRC-E), using an open acid digestion technique. Precision and accuracy were examined with international standard reference materials SDO-1, GSS-4, and SO-1. The error in XRF data ranges from 2 to 5% while that in ICP-MS is less than 5% (Ahmad et al. 2005; Rao and Rai 2006). The analyses for major oxides, trace elements, and rare earth elements of the rock samples are presented in Tables 1 and 2.

4 Results

4.1 Petrography

Microscopic study of representative thin sections of Surma and Barail sandstones showed that the rocks were medium to fine-grained, well sorted and sub-rounded to sub-angular in nature (Fig. 2a–d). The framework grains of the studied sandstones were composed of quartz (monocrystalline, Qm and polycrystalline, Qp), K-feldspar, plagioclase, and rock fragments with very minor presence of mica, chlorite, and

zircon. Quartz dominated feldspar and rock fragments in the sandstones of both the rock groups. There were no visible textural characteristic and mineral constituent differences between the sandstones of either group. The quartz grains were commonly sub-rounded to subangular in shape. Among quartz grains, Qm was dominant over Qp. Qm grains were mostly non-undulatory while a few were undulose in nature. Quartz grains were observed with concavo-convex contact, sutured contact, and straight contact boundary.

Feldspars are the second most abundant framework grains which make up 1–15% of the total grain population. Both plagioclase and K-feldspars are observed in the thin sections (Fig. 2a–d). Rock fragments observed in the studied thin sections are variable in size, angular to sub-angular, with prominent grain boundaries. They constitute 0–15% of the rock volume. Among micas, muscovite and biotite are observed in the thin section which are mostly detrital in origin but authigenic mica grains are also observed. Among heavy minerals, the most common is zircon, while in few samples rutile and sphene are also observed. Matrix is the common binding material for the framework grains. Matrix constitutes average 20% of the total rock volume.

4.2 Geochemistry

4.2.1 Major elements

The Barail sandstones are characterized by an average concentration of 76 wt% SiO₂, 11 wt% Al₂O₃, 5.5 wt%

Table 1 Whole-rock major and trace element analysis and Indices of alterations and weathering of sandstones of Barail Group, Mizoram Foreland Basin, Northeast India

Sample no.	SCZ 3	SCZ 4	SCZ 12	SCZ 14	SCT 7	SCT 8	SCT 11	SCT 12	PAAS	UCC
<i>Major oxides (wt%)</i>										
SiO ₂	75.81	81.59	74.79	77.67	70.69	74.25	78.34	75.01	62.80	66.00
Al ₂ O ₃	11.91	7.44	12.41	9.41	12.53	11.52	8.24	11.60	18.90	15.20
Fe ₂ O ₃	4.70	3.72	3.57	4.12	5.32	4.07	4.25	4.14	6.50	5.00
MnO	0.07	0.03	0.07	0.03	0.13	0.07	0.11	0.04	0.1	0.08
MgO	1.11	0.78	1.24	1.29	2.22	1.56	1.04	1.22	2.20	2.20
CaO	0.26	0.18	1.18	0.29	1.06	0.47	0.22	0.58	1.30	4.20
Na ₂ O	1.33	0.91	1.54	1.62	1.66	1.85	1.56	1.64	1.20	3.90
K ₂ O	1.20	0.89	1.74	1.41	1.95	1.74	0.83	1.56	3.70	3.40
TiO ₂	0.96	0.51	0.65	0.76	0.51	0.51	0.58	0.64	1.00	0.50
P ₂ O ₅	0.11	0.06	0.08	0.08	0.07	0.07	0.07	0.08	0.20	0.20
LOI	3.28	2.36	2.84	2.04	3.85	2.45	3.07	2.83		
Total	100.74	98.47	100.11	98.72	99.99	98.56	98.31	99.34		
SiO ₂ /Al ₂ O ₃	6.37	10.97	6.03	8.25	5.64	6.45	9.51	6.47	3.32	4.34
Al ₂ O ₃ /TiO ₂	12.41	14.59	19.09	12.38	24.57	22.59	14.21	18.13	18.90	30.40
K ₂ O/Na ₂ O	0.90	0.98	1.13	0.87	1.17	0.94	0.53	0.95	3.08	0.87
<i>Trace elements (ppm)</i>										
Sc	8.60	7.60	8.90	8.80	10.80	8.60	7.20	10.00	16.00	13.60
V	86.00	59.00	72.00	75.00	77.00	72.00	65.00	78.00	150.00	60.00
Cr	130.00	94.00	123.00	119.00	121.00	104.00	103.00	92.00	110.00	83.00
Co	60.00	12.00	11.00	12.00	18.00	12.00	79.00	13.00	23.00	17.00
Ni	21.00	28.00	27.00	33.00	61.00	34.00	31.00	25.00	55.00	20.00
Cu	8.00	13.00	7.00	10.00	17.00	10.00	10.00	10.00	50.00	25.00
Zn	45.00	38.00	37.00	38.00	61.00	40.00	38.00	45.00	85.00	71.00
Ga	10.00	9.00	10.00	11.00	12.00	11.00	11.00	13.00	20.00	–
Rb	46.00	34.00	58.00	51.00	77.00	61.00	33.00	61.00	160.00	112.00
Sr	35.00	52.00	71.00	55.00	98.00	85.00	38.00	57.00	200.00	350.00
Y	33.00	13.00	21.00	21.00	19.00	17.00	18.00	23.00	27.00	22.00
Zr	1069.00	147.00	306.00	295.00	147.00	134.00	315.00	305.00	210.00	190.00
Nb	24.00	9.00	13.00	13.00	9.00	7.00	12.00	13.00	19.00	25.00
Ba	324.00	151.00	280.00	220.00	335.00	308.00	182.00	228.00	650.00	550.00
Pb	24.00	22.00	21.00	22.00	21.00	21.00	23.00	22.00	20.00	20.00
Th	22.00	11.00	11.00	12.00	10.00	10.00	11.00	14.00	14.60	10.70
U	3.89	bdl	1.13	2.63	0.81	1.06	1.99	bdl	3.10	2.80
<i>Rare earth elements (ppm)</i>										
La	52.94	24.23	42.74	40.49	31.53	23.25	31.51	36.06	38.20	30.00
Ce	178.20	51.40	86.89	82.04	62.90	47.74	62.60	70.96	79.60	64.00
Pr	11.31	5.41	9.12	8.66	6.88	5.21	6.82	7.62	8.83	7.10
Nd	19.16	23.35	38.55	35.60	29.4	22.07	29.64	33.40	33.90	26.00
Sm	9.03	4.57	7.35	7.01	5.92	4.38	5.57	6.11	5.60	4.50
Eu	1.55	0.93	1.46	1.39	1.32	0.94	1.07	1.14	1.08	0.88
Gd	6.21	3.17	5.00	4.84	4.32	3.06	3.92	4.11	4.70	3.80
Tb	1.07	0.56	0.88	0.85	0.80	0.53	0.71	0.76	0.77	0.64
Dy	5.15	2.62	4.20	4.00	3.87	2.69	3.42	3.87	4.68	3.50
Ho	0.95	0.48	0.76	0.73	0.73	0.47	0.66	0.72	0.99	0.80
Er	2.55	1.30	2.05	1.95	1.94	1.29	1.76	2.02	2.85	2.30
Tm	0.37	0.19	0.29	0.28	0.28	0.18	0.25	0.30	0.41	0.33

Table 1 continued

Sample no.	SCZ 3	SCZ 4	SCZ 12	SCZ 14	SCT 7	SCT 8	SCT 11	SCT 12	PAAS	UCC
Yb	1.99	1.05	1.52	1.47	1.48	0.94	1.38	1.57	2.82	2.20
Lu	0.28	0.15	0.21	0.20	0.21	0.13	0.19	0.23	0.43	0.32
ΣREE	290.76	119.41	201.02	189.51	151.58	112.88	149.50	168.87	184.86	146.37
Eu/Eu*	0.60	0.71	0.70	0.69	0.76	0.75	0.67	0.66	0.64	0.63
<i>Weathering indices</i>										
CIA	75	73	72	67	65	67	68	68	69	46
CIW	82	80	81	75	73	75	74	76	81	52

PAAS (Post Archaean Australian Shale) and UCC (Upper Continental Crust) values are from Taylor and McLennan (1985)

Eu/Eu* = $2 \times \text{Eu}_{\text{N}} / (\text{Sm}_{\text{N}} + \text{Gd}_{\text{N}})$

LOI loss on ignition, bdl below detection limit, CIA chemical index of alteration, CIW chemical index of weathering

($\text{Fe}_2\text{O}_3 + \text{MgO}$), 0.64 wt% TiO_2 , 1.5 wt% Na_2O , 1.4 wt% K_2O , and 0.41 wt% CaO . Surma sandstones also do not differ much from the Barail sandstone and have average concentrations of 69 wt% SiO_2 , 14 wt% Al_2O_3 , 6.5 wt% ($\text{Fe}_2\text{O}_3 + \text{MgO}$), 0.61 wt% TiO_2 , 1.6 wt% Na_2O , 2.3 wt% K_2O , and 1.3 wt% CaO . The SiO_2 , Al_2O_3 and Fe_2O_3 concentrations of the Barail and Surma sandstones are similar to that of Upper Continental Crust (UCC) (Taylor and McLennan 1985). TiO_2 contents of both Surma and Barail sandstones are higher, whereas CaO , Na_2O , K_2O , and P_2O_5 contents of the sandstones are significantly lower, than UCC (Taylor and McLennan 1985). Concentration of MnO in Surma sandstone is much higher than UCC, while Barail sandstones have lower contents of MnO compared to UCC.

Clastic sedimentary rocks are generally composed of variable contents of aluminous clays (Al_2O_3) and quartz (SiO_2) and display typical negative correlation trends. Sediments with higher proportions of quartz plot at the highest SiO_2 and lowest Al_2O_3 concentrations, while those with higher proportions of clay minerals, e.g. illite, muscovite, chlorite etc. plot at the highest Al_2O_3 and lowest SiO_2 . Barail and Surma sandstones define a singular linear negative correlation trend in the SiO_2 versus Al_2O_3 plot (Fig. 3), in which common minerals of clastic sedimentary rocks like K-feldspar, illite, and quartz are also plotted following Raza et al. (2012a, b) to contrast the chemical nature of the sediments. Both the Barail and Surma sandstones plotted in the intermediate position in the linear array in the diagram suggesting a mixture of quartz and illite end members (Fig. 3) or limited weathering condition of the sediments. In order to assess the control of clay minerals on the overall major elemental variations, K_2O , TiO_2 , Na_2O , MgO , CaO , Fe_2O_3 of both Barail and Surma sandstones are plotted on Harker variation diagram against Al_2O_3 (Fig. 4). The variation diagrams display strong

positive correlation for K_2O , TiO_2 and MgO against Al_2O_3 for both Barail and Surma sandstones. The positive correlation between Al_2O_3 and K_2O in the sandstones indicates the control of clay minerals such as illite, and/or presence of alkali feldspar. Positive correlation between Al_2O_3 and TiO_2 indicates the association of TiO_2 -bearing phases with the clay fraction or presence of fine-grained Ti-bearing heavy minerals in the sandstones. Na_2O and CaO contents of both Barail and Surma samples, however, display poor correlation with Al_2O_3 (Fig. 4). In the $\text{Fe}_2\text{O}_3/\text{K}_2\text{O}$ versus $\text{SiO}_2/\text{Al}_2\text{O}_3$ chemical classification diagram of Herron (1988), the studied samples plot around wackes field with certain variability (Fig. 5a). In the $\text{SiO}_2/\text{Al}_2\text{O}_3$ versus $\text{Na}_2\text{O}/\text{K}_2\text{O}$ classification diagram of Pettijohn et al. (1972) (Fig. 5b) the studied sandstones plot confined within the litharenite field while few Surma samples plot within the field of greywacke as well.

4.2.2 Trace element geochemistry

Barail and Surma sandstones have lower Large Ion Lithophile Elements (LILE) (Rb, Sr, Ba) and transition elements (Sc, V, Ni, Cu, Zn) concentrations compared to UCC (Taylor and McLennan 1985) and Post Archean Australian Shale (PAAS) (Taylor and McLennan 1985). However, Cr and Zr show higher concentrations than the standards (Tables 1, 2). Surma sandstones are characterized by higher concentrations of Rb (avg. 94 ppm), Sr (88 ppm), Ba (349 ppm), and Cr (162 ppm) compared to Barail sandstones (Rb = 53 ppm; Sr = 61 ppm; Ba = 254 ppm; Cr = 111 ppm). Barail sandstones however have higher Zr (average 340 ppm) concentration compared to Surma sandstones (Zr average = 202 ppm). Surma and Barail sandstones bear similar concentrations of immobile High Field Strength Elements (HFSE) (Nb, Y, Th, U) (Tables 1, 2). While plotted against Al_2O_3 , certain trace

Table 2 Whole-rock major and trace element analysis and Indices of alterations and weathering of sandstones of Surma Group, Mizoram Foreland Basin, Northeast India

Sample no.	SAR 5	SAS 5	SAT 2	SAZ 3	SBD 7	SCT 23	SCT 57	SCT 60	SCT 62	SVC 7
<i>Major oxides (wt%)</i>										
SiO ₂	61.98	61.62	75.00	74.59	77.13	71.22	68.88	68.25	72.11	61.40
Al ₂ O ₃	17.40	17.18	10.78	11.13	9.91	12.58	13.33	15.53	14.01	19.35
Fe ₂ O ₃	5.02	5.05	4.27	3.84	3.67	4.13	3.75	4.86	4.04	6.41
MnO	0.13	0.30	0.05	0.03	0.09	0.16	0.08	0.06	0.05	0.17
MgO	2.23	2.32	1.58	1.46	0.80	2.41	2.29	2.68	2.34	2.22
CaO	2.78	3.32	0.69	0.31	0.35	0.98	2.41	0.95	0.42	0.60
Na ₂ O	1.35	1.26	1.81	1.68	1.44	1.60	1.53	1.69	2.07	1.23
K ₂ O	3.03	2.53	1.99	1.93	1.50	1.87	2.27	2.53	2.22	3.38
TiO ₂	0.65	0.71	0.48	0.65	0.63	0.64	0.52	0.64	0.46	0.68
P ₂ O ₅	0.12	0.12	0.11	0.08	0.09	0.09	0.11	0.10	0.07	0.12
LOI	5.52	5.52	3.43	2.41	3.32	4.04	4.76	3.49	3.02	5.22
Total	100.21	99.93	100.19	98.11	98.93	99.72	99.93	100.78	100.81	100.78
SiO ₂ /Al ₂ O ₃	3.56	3.59	6.96	6.70	7.78	5.66	5.17	4.39	5.15	3.17
Al ₂ O ₃ /TiO ₂	26.77	24.20	22.46	17.12	15.73	19.66	25.63	24.27	30.46	28.46
K ₂ O/Na ₂ O	2.24	2.01	1.10	1.15	1.04	1.17	1.48	1.50	1.07	2.75
<i>Trace elements (ppm)</i>										
Sc	12.70	13.00	8.70	9.70	8.50	9.23	9.40	10.80	7.40	14.70
V	92.00	89.00	68.00	74.00	66.00	71.00	65.00	85.00	64.00	112.00
Cr	302.00	118.00	265.00	180.00	119.00	107.00	119.00	181.00	89.00	144.00
Co	16.00	36.00	11.00	11.00	10.00	63.00	51.00	16.00	67.00	19.00
Ni	46.00	43.00	32.00	25.00	27.00	29.00	42.00	49.00	42.00	46.00
Cu	20.00	16.00	8.00	8.00	9.00	11.00	10.00	14.00	12.00	30.00
Zn	64.00	65.00	32.00	41.00	35.00	44.00	46.00	58.00	43.00	84.00
Ga	15.00	15.00	11.00	12.00	12.00	12.00	12.00	14.00	12.00	19.00
Rb	141.00	106.00	73.00	71.00	54.00	68.00	86.00	106.00	79.00	160.00
Sr	109.00	152.00	105.00	58.00	57.00	57.00	76.00	85.00	83.00	95.00
Y	29.00	26.00	21.00	23.00	24.00	20.00	22.00	26.00	18.00	34.00
Zr	203.00	168.00	200.00	333.00	157.00	245.00	158.00	222.00	125.00	207.00
Nb	11.00	11.00	9.00	12.00	11.00	12.00	8.00	11.00	8.00	12.00
Ba	427.00	347.00	298.00	310.00	313.00	288.00	297.00	358.00	354.00	495.00
Pb	23.00	22.00	22.00	22.00	22.00	22.00	21.00	22.00	21.00	28.00
Th	14.00	10.00	12.00	15.00	13.00	12.00	9.00	12.00	10.00	17.00
U	0.83	1.76	bdl	1.57	2.43	1.88	bdl	4.19	1.66	2.40
<i>Rare earth elements (ppm)</i>										
La	43.55	30.54	30.51	48.40	42.75	28.44	25.20	37.69	30.93	30.93
Ce	84.32	59.49	60.48	95.89	84.37	55.94	47.94	73.91	60.56	63.98
Pr	9.07	6.44	6.64	9.95	9.18	5.96	5.47	7.88	6.55	6.52
Nd	38.19	27.44	26.83	41.05	39.02	25.70	23.76	33.06	27.21	26.68
Sm	7.25	5.49	5.34	7.79	7.98	4.69	4.70	6.43	5.25	5.36
Eu	1.41	1.18	1.01	1.45	1.65	0.89	0.96	1.22	1.08	1.11
Gd	4.99	3.99	3.86	5.43	5.86	3.16	3.51	4.37	3.54	3.95
Tb	0.88	0.77	0.68	0.96	1.06	0.57	0.68	0.80	0.65	0.69
Dy	4.25	3.78	3.34	4.48	5.22	2.78	3.71	4.14	3.36	3.41
Ho	0.78	0.71	0.61	0.82	0.97	0.53	0.70	0.78	0.63	0.66
Er	2.16	1.95	1.74	2.19	2.54	1.44	1.92	2.13	1.76	1.83
Tm	0.31	0.27	0.25	0.31	0.35	0.21	0.27	0.31	0.26	0.26

Table 2 continued

Sample no.	SAR 5	SAS 5	SAT 2	SAZ 3	SBD 7	SCT 23	SCT 57	SCT 60	SCT 62	SVC 7
Yb	1.64	1.44	1.36	1.61	1.91	1.14	1.42	1.63	1.41	1.40
Lu	0.23	0.20	0.19	0.23	0.27	0.16	0.20	0.23	0.20	0.20
Σ REE	199.03	143.69	142.84	220.56	203.13	131.61	120.44	174.58	143.39	146.98
Eu/Eu*	0.68	0.74	0.65	0.65	0.71	0.67	0.70	0.67	0.73	0.70
<i>Weathering indices</i>										
CIA	68	71	63	67	68	66	65	68	68	74
CIW	77	81	72	77	77	74	72	78	77	86

CIA chemical index of alteration, CIW chemical index of weathering, bdl below detection limit

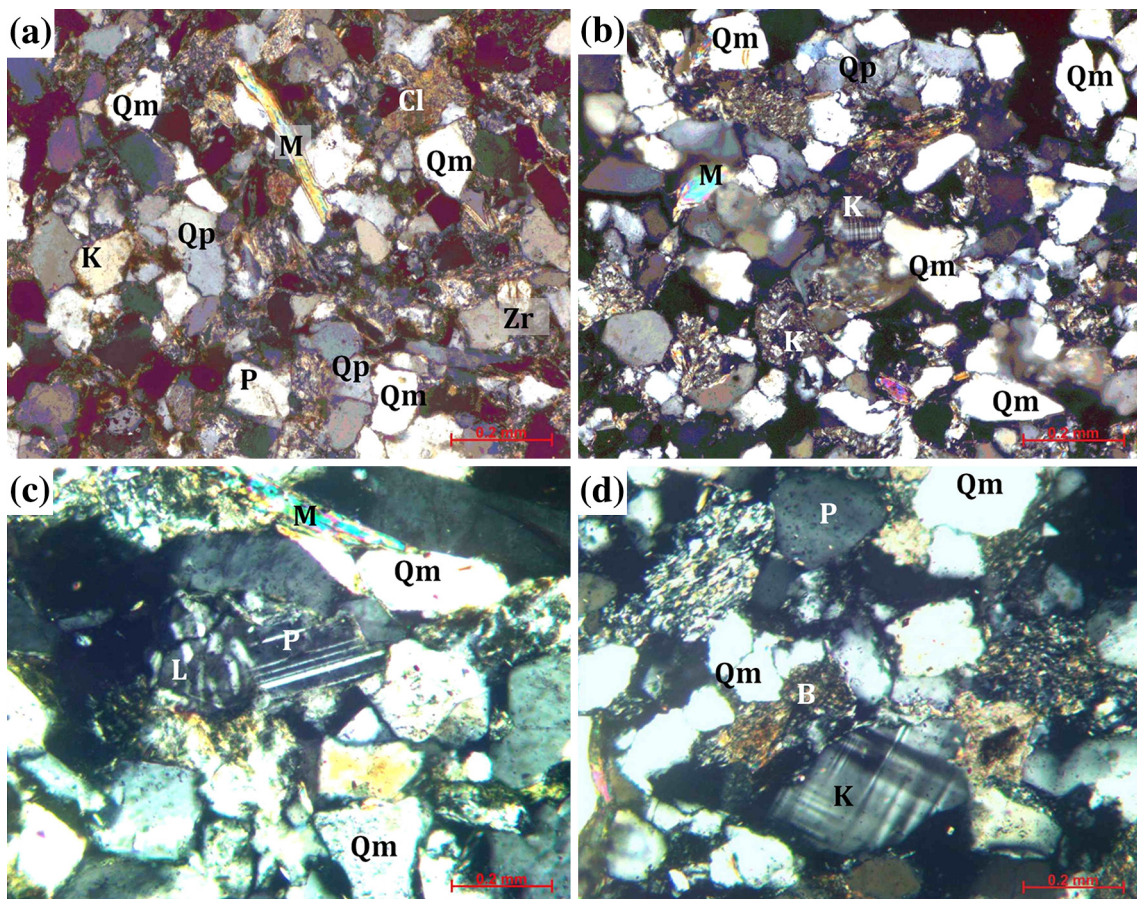


Fig. 2 Photomicrographs of representative sandstones from Barail (a, b) and Surma Groups (c, d) showing the textural characteristics and different minerals and rock fragments present. Qm, monocrystalline quartz; Qp, polycrystalline quartz; K, K-feldspar; P, plagioclase; L, lithic grains; Ch, chlorite; Zr, zircon; M, Muscovite; B, Biotite. The framework mineral grains of both Barail and Surma sandstones are medium to coarse-grained, sub-angular to sub-rounded and are moderately well sorted. There are dominances of monocrystalline quartz over polycrystalline variety in the sandstones of both the rock groups

elements like Rb, Sr, Ba, Th, Ni, V, and Y of the studied sandstones of Barail and Surma Groups displayed moderate positive correlations (Fig. 6a, b) and few other trace elements like Zr, Cr, Co, and Nb of the studied sandstones showed poor correlation (Fig. 6a, b). The total Rare Earth

Element contents (Σ REE) of Surma sandstone showed poor correlation with Al_2O_3 , however Barail sandstones shows weak positive correlations between (Σ REE) and Al_2O_3 (Fig. 6a). On intense chemical weathering of a source rock, the immobile elements show strong and positive

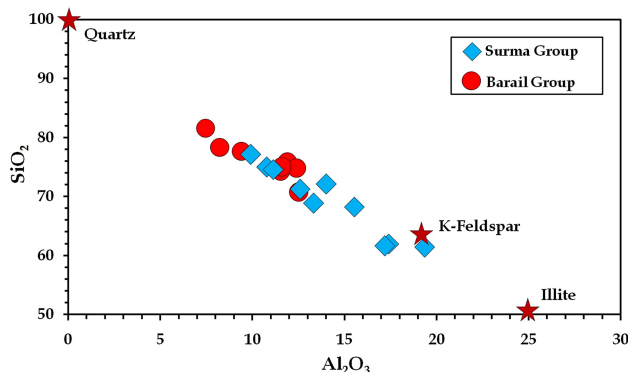


Fig. 3 Al_2O_3 versus SiO_2 plot of Barail and Surma Group sandstones from Mizoram Foreland Basin, Northeast India. Stars are the common minerals of clastic sedimentary rocks e.g. Illite, K-feldspar and Quartz (as plotted by Raza et al. 2012a, b)

correlation with Al_2O_3 (Young and Nesbitt 1998). The observed geochemical characteristics therefore indicate that the sediments were derived from a source which had undergone limited chemical weathering.

4.2.3 Rare earth element geochemistry

Total REE (ΣREE) concentrations in the Surma sandstones (ranges from 120 to 221 ppm; average 163 ppm) were similar to those observed in Barail sandstone (ranges from 113 to 291 ppm; average 173 ppm). The studied sandstones had higher REE abundances compared to UCC but had lower REE abundances than PAAS (values after Taylor and McLennan 1985). Chondrite normalized rare earth elements patterns for Surma and Barail sandstones displayed enrichment of Light Rare Earth Elements (LREE: La-Gd), fractionated Heavy Rare Earth Elements (HREE: Tb-Lu), and negative Eu anomaly (average $\text{Eu}/\text{Eu}^* = 0.69$) (Fig. 7a, b). The REE patterns of the sandstones were uniform and relatively similar to UCC. The highly fractionated REE patterns for the sandstones [Surma: $(\text{La/Lu})_N = 13.35\text{--}22.04$; Barail: $(\text{La/Lu})_N = 15.59\text{--}21.13$], therefore, suggest that the detritus were probably derived from an igneous rocks of Upper Continental Crust.

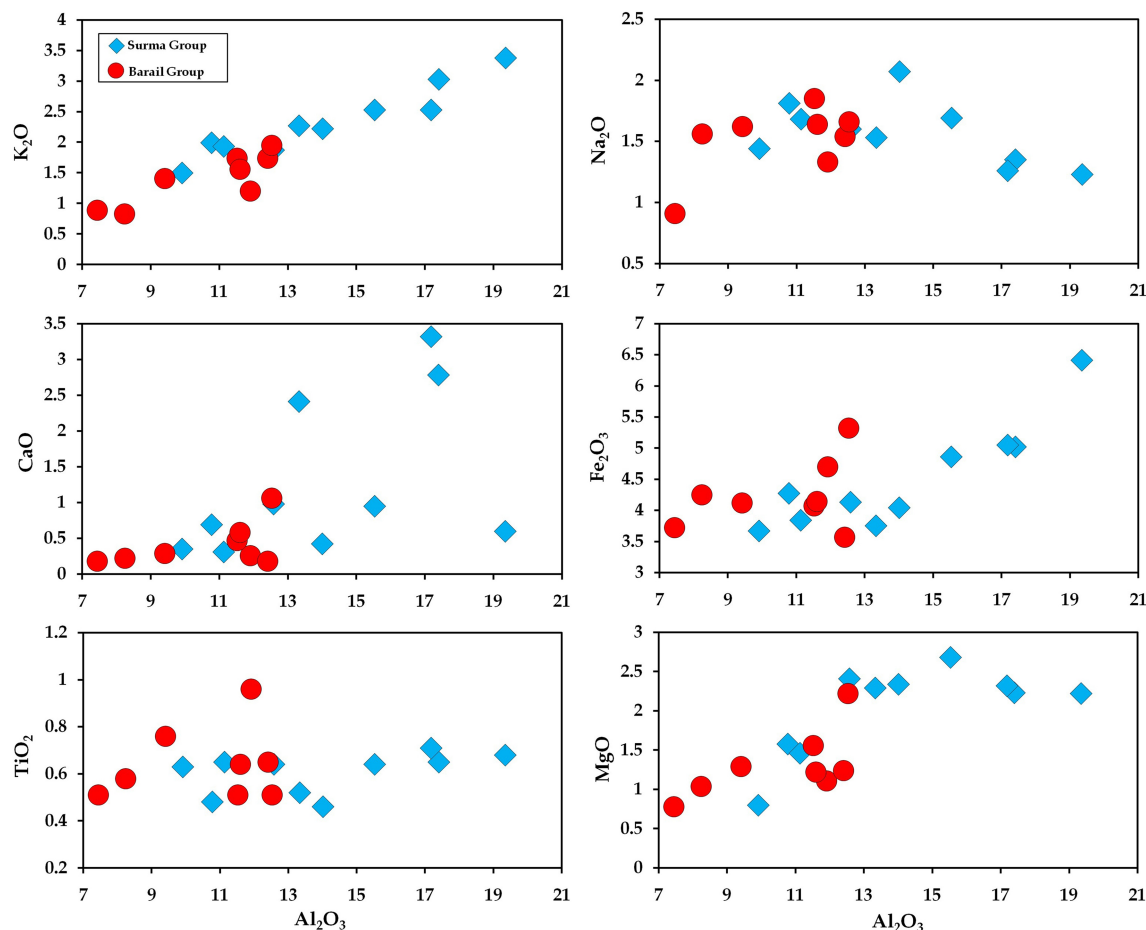


Fig. 4 Bivariate diagram for oxides of major element versus Al_2O_3 for the sandstones from Barail and Surma Groups

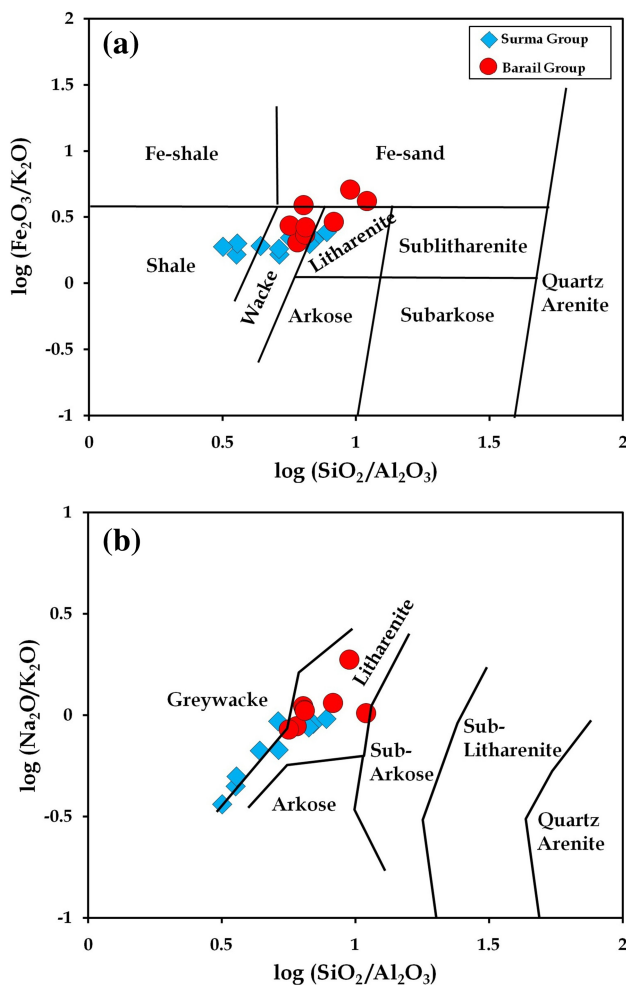


Fig. 5 Chemical classification of Barail and Surma sandstones based on **a** $\log(\text{SiO}_2/\text{Al}_2\text{O}_3)$ versus $\log(\text{Fe}_2\text{O}_3/\text{K}_2\text{O})$ diagram of Herron (1988) and **b** $\log(\text{SiO}_2/\text{Al}_2\text{O}_3)$ versus $\log(\text{Na}_2\text{O}/\text{K}_2\text{O})$ diagram of Pettijohn et al. (1972)

5 Discussion

5.1 Paleoweathering and sediment recycling

In order to evaluate qualitatively and quantitatively the paleoclimatic conditions and the degree of source rock weathering, Chemical Index of Alteration (CIA; Nesbitt and Young 1982) [$\text{CIA} = \text{Al}_2\text{O}_3/(\text{Al}_2\text{O}_3 + \text{CaO}^* + \text{Na}_2\text{O} + \text{K}_2\text{O}) \times 100$], Chemical Index of Weathering (CIW; Harnois 1988) [$\text{CIW} = \text{Al}_2\text{O}_3/(\text{Al}_2\text{O}_3 + \text{CaO}^* + \text{Na}_2\text{O}) \times 100$], etc. have long been used (Armstrong-Altrin et al. 2004; Nagarajan et al. 2007; Bhuiyan et al. 2011; Sun et al. 2012; Ramachandran et al. 2016). CaO^* indicates Ca incorporated from the silicate bearing minerals and it was calculated using following assumptions: a) if the CaO content was less or equal to the Na_2O content, then the CaO value was considered same as CaO^* value and b) if the CaO content was higher than Na_2O , then Na_2O value was

considered as CaO^* value (Bock et al. 1998; Gallet et al. 1998; Roddaz et al. 2006). Fresh and un-weathered igneous rocks are characterized by CIA values of 50 or less, whereas intense weathering produces residual clay with kaolinite and gibbsite in the residual clay and results in CIA values close to 100. CIA values of 70 to 75 indicate moderate chemical weathering and the formation of muscovite, illite, and smectite during weathering of the source. The CIA value for Surma sandstone varies from 63 to 74 and averages 68, and the Barail sandstone ranges from 65 to 75 and averages 69, suggesting the sediments for both Surma and Barail Groups might have been derived from a moderately weathered source as compared to the average shale (CIA: 70–75, Taylor and McLennan 1985). Previous studies on the Surma and Barail sandstones of Bengal basin also provide similar CIA values (see e.g., Rahman and Suzuki 2007; Hossain et al. 2010; Rahman et al. 2014) and are interpreted to have been derived from a mild to moderately weathered source. Although CIA is considered as one of the important indices to measure the extent of weathering, but remobilization of K during the sedimentation and metamorphic processes can produce spurious CIA values. Harnois (1988) proposed the use of Chemical Index of Weathering (CIW) as an alternative index which excludes potassium in the formula of CIA. The CIW values for the Surma sandstones varies from 72 to 86, and that of Barail sandstones varies from 73 to 82, indicating that the Surma and Barail sediments were derived from a moderately weathered source.

Large sedimentary basins are subjected to several cycles of sedimentation; the detritus of each cycle were produced by variable intensities of weathering. The geochemical composition of the clastic sedimentary rocks thus bears the imprints of several previous weathering conditions. It therefore becomes imperative to analyze the sediment recycling in order to decipher whether the geochemical composition of the sediments was modified during the sedimentary transport from the source to the basin or it reflects source characteristics. The average CIA (Barail: 69; Surma: 68) and CIW (both Barail and Surma: 77) values of the studied sandstones imply that their precursor sediments did not suffer from strong chemical weathering conditions. In this regard, Rb/Sr and Th/U ratios are generally quite helpful to understand the effects of sediment recycling. Sr is a mobile element under certain conditions. Weathering can therefore result in an obvious increase of the Rb/Sr ratio of sedimentary rocks. An Rb/Sr ratio of > 0.5 suggests strong weathering and sedimentary recycling (McLennan et al. 1993). The average Rb/Sr ratios of the Barail and Surma Group samples were 0.89 and 1.11 respectively and therefore suggest the sediments were affected by recycling up to certain degrees. Besides, increase in the intensity of weathering of source rocks,

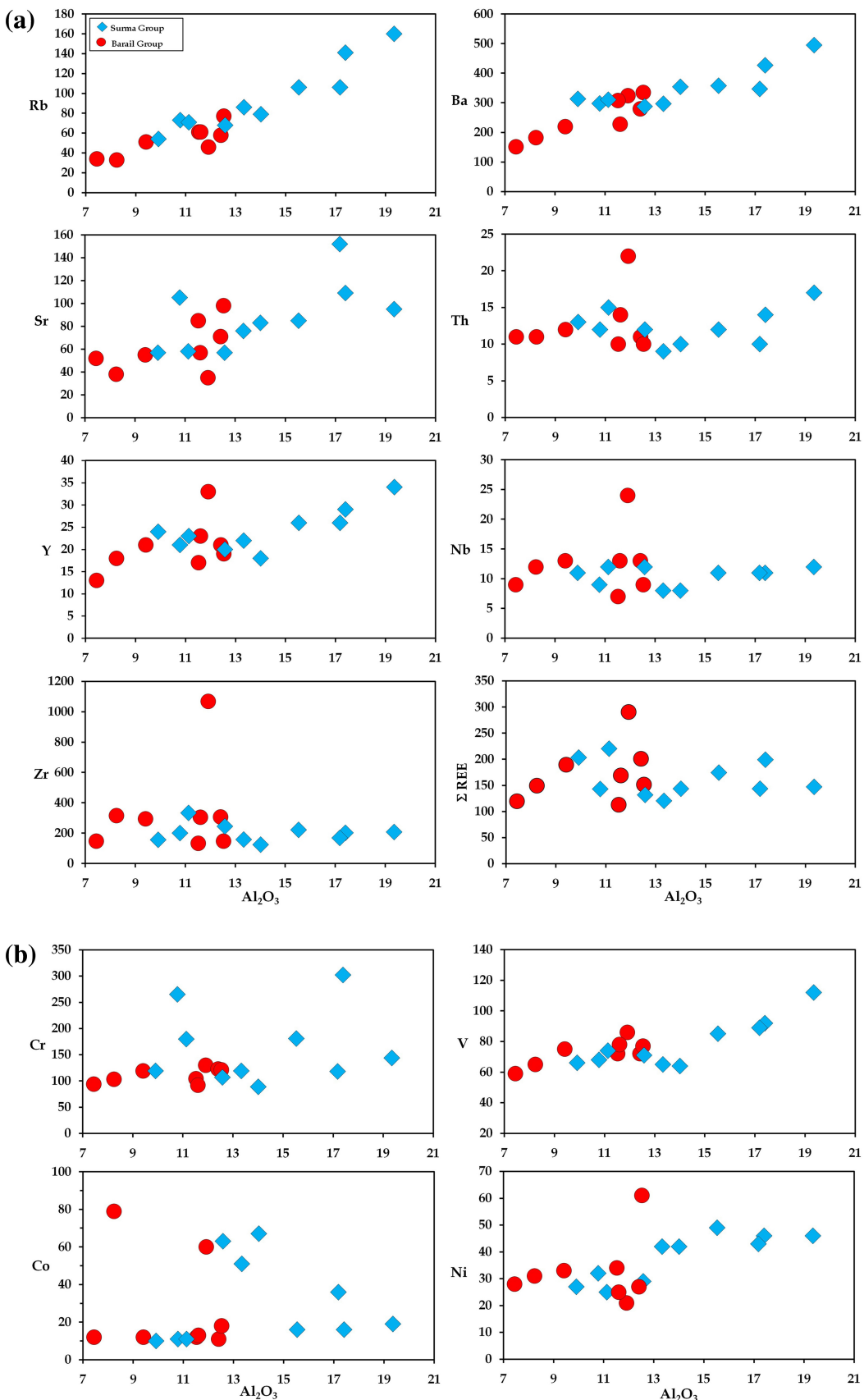


Fig. 6 Bivariate diagrams for **a** incompatible trace elements versus Al_2O_3 and **b** transition elements versus Al_2O_3 for the sandstones from Barail and Surma Groups

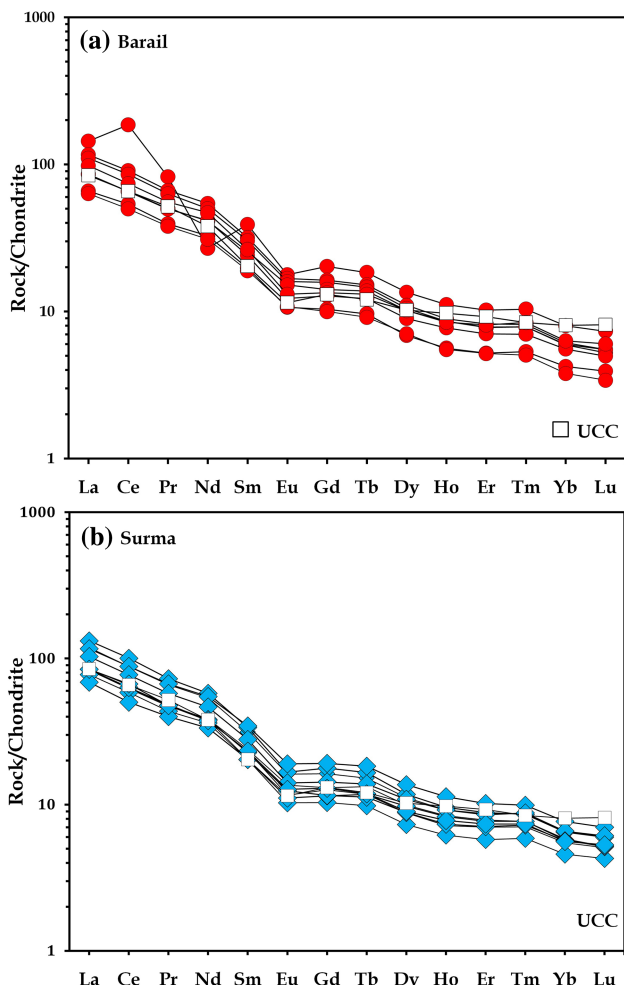


Fig. 7 Chondrite-normalized (values after Taylor and McLennan 1985) Rare Earth Element patterns for **a** Barail sandstones and **b** Surma sandstones. UCC composition (values after Taylor and McLennan 1985) is plotted with the sandstone data for comparison

results in an increase of Th/U ratio (McLennan 2001). Th/U ratio above the upper crustal values ($\text{Th}/\text{U} = 3.5\text{--}4$, McLennan et al. 1993) indicates certain degrees of recycling of sediments. The Th/U ratios of the studied sandstones average 7.88 for Barail Group and 7.48 for Surma Group, which are higher than the average Th/U ratio of the upper crust, suggests certain degrees of recycling of sediments over the transport and sedimentary processes. Limited scale of recycling of the precursor sediments for the Barail sandstones in particular, is also manifested in the Th/Sc versus Zr/Sc diagram of McLennan et al. 1993 (Fig. 9; discussed later in Sect. 5.2). Zr/Sc ratio is

considered as an index of heavy mineral enrichment including zircon which increases significantly during sediment recycling (McLennan 1989). Barail and Surma sandstones show moderately variable Zr/Sc ratios (Surma: 12.92–34.33; Barail: 13.61–124.30) at more or less uniform Th/Sc ratios (Surma: 0.77–1.55; Barail: 0.93–2.56). A majority of the studied samples plot on the left of the magmatic compositional variation trend of rocks in the Th/Sc versus Zr/Sc diagram (Fig. 9), except few Barail samples, which plot to the right of the compositional trend with higher Zr/Sc ratios suggesting zircon enrichment during recycling.

Besides the zircon enrichment during sedimentary sorting, enrichment of some other accessory minerals, like apatite, would also have an effect on the bulk rock geochemical compositions (Wang and Zhou 2013). Sorting and enrichment of common heavy minerals, such as zircon, apatite, and monazite, may erratically affect REE patterns of bulk-rock samples due to their different partition coefficients for LREE and HREE (Wang and Zhou 2013 and references therein). Poor correlation between $(\text{La}/\text{Yb})_{\text{N}}$ and P_2O_5 (wt%), (figure not shown) of the Barail and Surma sandstones suggests that the bulk chemical composition including the REE pattern of the studied rocks is not affected by sorting of monazite and/or apatite.

5.2 Provenance

Geochemical data of clastic sediments has long been used for determining provenance (see e.g. Floyd and Leveridge 1987; Cullers 1995; Armstrong-Altrin et al. 2004 and 2013). $\text{Al}_2\text{O}_3/\text{TiO}_2$ ratios in the sedimentary rocks offer an important clue to decipher the types of source rocks (Garcia et al. 1994; Hayashi et al. 1997; Andersson et al. 2004). During weathering of source rocks, Al and Ti remain essentially immobile, and therefore the values of $\text{Al}_2\text{O}_3/\text{TiO}_2$ ratios of residual detritus can be considered as source characteristics. In magmatic rocks, Al occurs mostly in feldspars and Ti in mafic minerals (e.g. pyroxene, hornblende, biotite, rutile, ilmenite). Therefore, the $\text{Al}_2\text{O}_3/\text{TiO}_2$ and SiO_2 increase sympathetically in magmatic rocks (Hayashi et al. 1997). Sediments which are sourced from mafic rocks, have $\text{Al}_2\text{O}_3/\text{TiO}_2$ ratio value < 14 , and those which sourced from felsic rocks, have $\text{Al}_2\text{O}_3/\text{TiO}_2$ ratio value in the range of 19–28 (Hayashi et al. 1997). $\text{Al}_2\text{O}_3/\text{TiO}_2$ ratios in the Surma sandstones vary from 15.73 to 30.46 (Table 2) while the Barail sandstones show the ratios ranging from 12.41 to 24.57 (Table 1) suggesting the sediments were derived predominantly from felsic sources.

In order to estimate the bulk source rock composition, a molecular proportion of $\text{Al}_2\text{O}_3\text{--CaO} + \text{Na}_2\text{O}\text{--K}_2\text{O}$ (A-CN-K) ternary plot of Nesbitt and Young (1984) was used (Fig. 8). Experimental and observational evidences suggest

sediments derived from less weathered source rocks follow trend parallel to the A-CN line originating from granodiorite or UCC (Fig. 8). Intense weathering leaches CaO and Na₂O totally and transforms the feldspars into illite, and the sediment's composition plots closer to the A-K join and the illite composition in the A-CN-K space (Nesbitt and Young 1984; Fig. 8). Extreme weathering of the source rocks produces kaolinite and curves the weathering trend towards the Al₂O₃ apex when approaching the A-K join (Nesbitt and Young 1984). The studied samples plot along the ideal weathering line for granodiorite in the A-CN-K diagram (Fig. 8). Data for probable Himalayan source rocks as well as the field of coeval Siwalik sediments (after Roy and Roser 2013, and references therein) are also plotted in the diagram. Barail and Surma sediments plot confined within the field of Siwalik sediments in the A-CN-K diagram and collinear with Surma sandstone data falling at the lower end of the distribution along the trend which appears originate from a source in close proximity with the composition of Trans-Himalayan granitoids (Fig. 8). Similar observations have also been made by Roy and Roser (2013), while working with the Tertiary NW shelf sandstones of Bengal basin.

Th/Sc versus Zr/Sc plot (Fig. 9) is very popularly used for provenance study of clastic sedimentary rocks in addition to assess sediment recycling (McLennan et al.

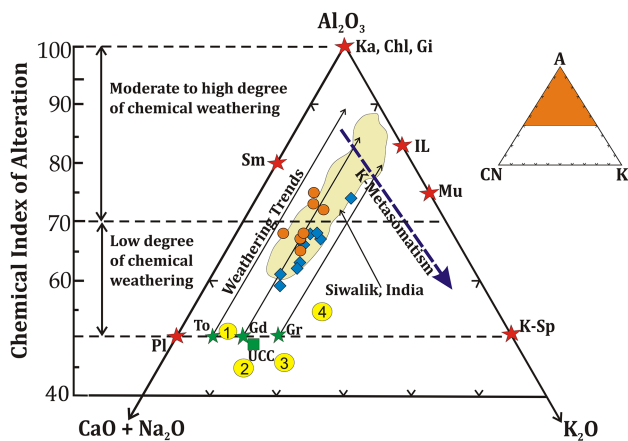


Fig. 8 A-CN-K ternary diagram (after Nesbitt and Young 1984) for Surma and Barail sandstones of Mizoram Foreland Basin. A = Al₂O₃, CN = CaO + Na₂O, K = K₂O (molecular proportions), Ka = kaolinite, Chl = chlorite, Gi = gibbsite, Mu = muscovite, Plag = plagioclase, K-sp = K-feldspar, Sm = smectite. Data for tonalite (To), granodiorite (Gd) and granite (Gr) are from Condie (1993). Arrows parallel to the A-CN edge are the weathering trends of To, Gd and Gr. Symbols are as in Fig. 5. Data for probable Himalayan source rocks are plotted as numbers in circles: (1) Cretaceous granitoids (Trans-Himalaya-Ladakh; Sharma et al. 2011); (2) Trans-Himalayan batholiths (Galy and France-Lanord 2001); (3) Tertiary leucogranite (Higher Himalaya; Sharma et al. 2011); (4) Palaeozoic granitoids (Lesser Himalaya, Mandi-granite; Sharma et al. 2011). Field for the Siwalik Group, NW Himalaya, India (Ranjan and Banerjee 2009) is also plotted (after Roy and Roser 2013) for comparison

1993). Th is an incompatible element and is enriched in silicic rocks, while Sc is a compatible element and is enriched in basic rocks. The ratio is not much affected during sedimentary recycling processes (McLennan et al. 1993; Cullers 1994a). The studied sandstones form a relatively tight group, which is slightly inclined to the compositional trend defined by volcanic rocks ranging from basalt to rhyolite (data after Taylor 1965, 1969). The studied samples plot clustered around Tonalite-Trondjemite-Granodiorite (TTG) composition and also plot confined within the field of Siwalik sediments (after Roy and Roser 2013) (Fig. 9), suggesting the provenance for both the Surma and Barail sandstones was largely singular. Certain other elemental ratios e.g. Eu/Eu*, La_N/Lu_N, La/Sc, La/Co, Th/Sc, Th/Co, and Cr/Th are also widely used for assessing the source rock composition of clastic sedimentary rocks (see e.g. Armstrong-Altrin et al. 2004; Armstrong-Altrin 2009; Cullers 2000, 2002; Tijani et al. 2010; Konstantopoulos and Zelilidis 2012). The values of Eu/Eu*, (La_N/Lu_N), La/Sc, La/Co, Th/Sc, Th/Co, and Cr/Th ratios of the studied rocks are presented in Table 3 along with those from the UCC, PAAS, and from sediments derived from mafic and felsic rocks. The value of these elemental ratios in the studied rocks match well with the sediments derived from felsic rocks.

The REE patterns and size of Eu anomaly in the sedimentary rocks have also been utilized to infer the nature of source rocks (Taylor and McLennan 1985; Armstrong-

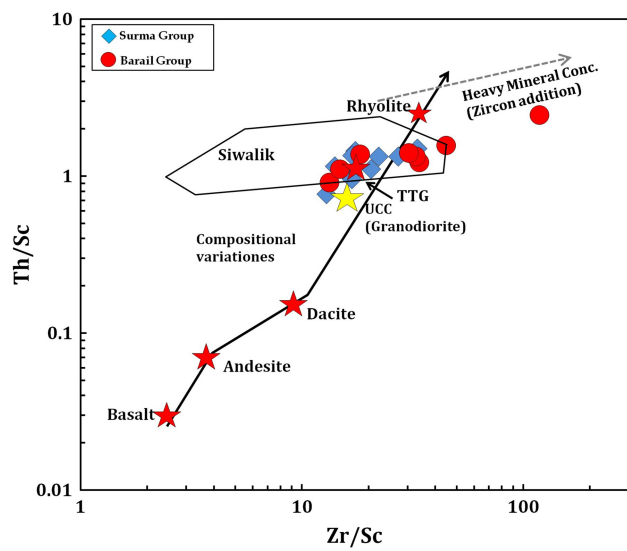


Fig. 9 Th/Sc versus Zr/Sc plot for the sandstones of Surma, Barail Groups of Mizoram Foreland Basin (after McLennan et al. 1993). Stars: basalt, andesite and rhyolite are average volcanic rock compositions (as plotted by Roser and Korsch 1999). Solid arrow is the compositional trend; dashed arrow indicates trends expected for zircon concentration. Field: Siwalik Group, NW Himalaya, India (as plotted by Roy and Roser 2013 with data from Ranjan and Banerjee 2009)

Table 3 Range of certain Trace and REE elemental ratios of sandstones in this study compared to the ratios in similar fractions in sediments derived from felsic rocks, mafic rocks, UCC and PAAS

Elemental ratio	Barail group ^a	Surma group ^a	Felsic sources ^b	Mafic sources ^b	UCC ^c	PAAS ^c
La/Sc	2.70–6.16	2.10–5.03	2.50–16.3	0.43–0.86	2.21	2.39
La/Co	0.40–3.89	0.45–4.40	1.80–13.8	0.14–0.38	1.76	1.66
Th/Sc	0.93–2.56	0.77–1.55	0.84–20.5	0.05–0.22	0.79	0.91
Th/Co	0.14–1.08	0.15–1.36	0.67–19.4	0.04–1.40	0.63	0.63
Cr/Th	5.91–12.10	8.47–22.08	4.00–15.0	25–500	7.76	7.53
Eu/Eu*	0.60–0.76	0.65–0.74	0.40–0.94	0.71–0.95	0.63	0.64
La _N /Lu _N	15.59–21.13	13.35–22.04	3.00–27.0	1.10–7.00	9.73	9.22

^aThis study; ^bFelsic and Mafic Sources: Cullers (1994a, b, 2002), Cullers and Podkrovov (2002), ^cTaylor and McLennan (1985)

Altrin 2009; Madhavaraju and Lee 2010; Armstrong-Altrin et al. 2013). Felsic rocks, in general, show a higher LREE/HREE ratio and exhibit negative Eu anomalies, while mafic rocks show a low LREE/HREE ratio with or without Eu anomalies (Cullers et al. 1987; Cullers 1994a, b). The studied Surma and Barail samples display fractionated chondrite-normalized REE patterns, negative Eu anomalies (Eu/Eu*: Barail = 0.60–0.76; average 0.69 and Surma = 0.65–0.74; average 0.69; Table 3), LREE enriched, and flat HREE patterns (Fig. 7a, b). Such REE patterns suggest that the sediments were probably derived from an evolved crustal source.

Surma samples additionally display MnO contents one order of magnitude higher than Barail samples (Tables 1, 2). Besides, the Sc, V, Co, and Ni contents of the Surma sandstones are also slightly higher than those of Barail sandstones (Tables 1, 2). These features point towards a certain quantity of mafic detrital input in Surma sediments. In the Co/Th versus La/Sc diagram of Gu et al. (2002) (Fig. 10) despite their compositional variability, few Surma samples plot closer to andesite values (Condie 1993) than those of the Barail Group samples, suggesting certain degree of influence of mafic sources on the detritus of the Surma sandstones.

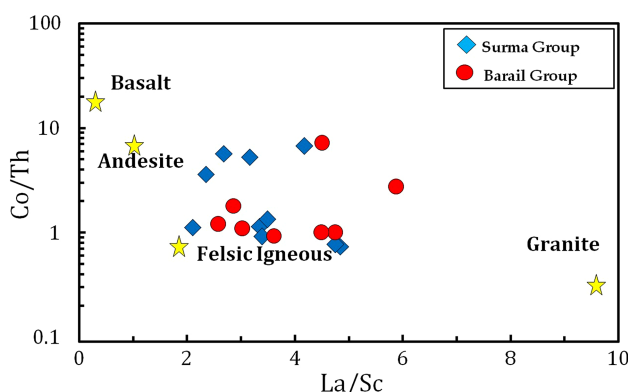


Fig. 10 La/Sc versus Co/Th plot for Surma and Barail sediments (after Gu et al. 2002). Stars are average basalt, andesite, granite and felsic igneous rock with data from Condie (1993)

There are several coeval Himalayan foreland basins in which Cenozoic sediments were deposited and their provenance has been deciphered e.g. Assam Basin by Cina et al. (2009); Bengal Basin by Najman et al. (2008), Indo-Burman Ranges (IBR) by Allen et al. (2008); Central Myanmar Basin by Robinson et al. (2014). The synorogenic Cenozoic sediments were derived by erosion of multiple sources including cratonic India, Neoproterozoic-Cambrian to Eocene Tethyan Himalayan Sequence (THS), Neoproterozoic to Cambrian Higher Himalayan Crystallines (HHC), Gangdese arc and the Late Cretaceous-Eocene eastern Trans-Himalayan batholiths (ETB) and other eastern Himalayan lithotectonic units in different proportions (Vadlamani et al. 2015; and references therein). Although

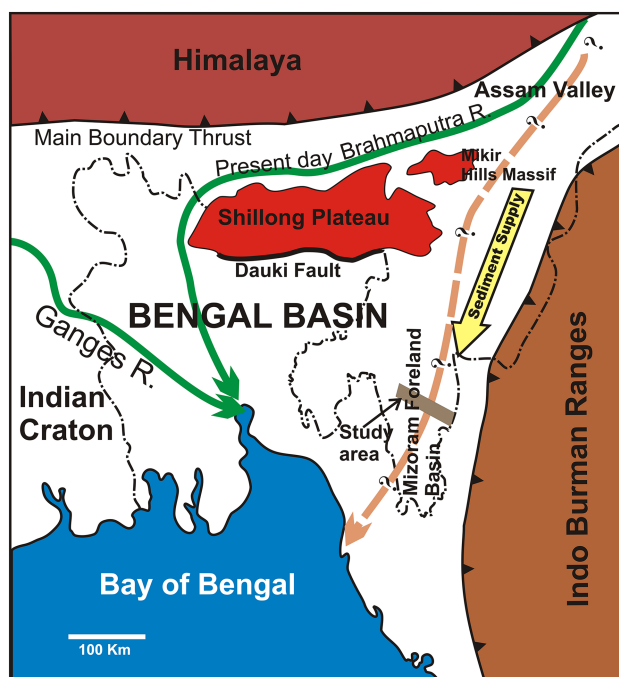


Fig. 11 Map showing a probable paleo-course of Brahmaputra River during early Miocene (modified after Uddin and Lundberg 1999) in red dotted line in the east of Shillong Plateau along with the present day course of river Brahmaputra flowing north of Shillong plateau

there are no U–Pb detrital zircon age data available on the sediments of MFB. However, the coeval Cenozoic sediments of adjacent Assam Foreland Basin (AFB) which were geochronologically studied by Vadlamani et al. (2015) can be correlated. The U–Pb ages of detrital zircons from the Oligocene Barail Group of Assam foreland basin were probably sourced from the Gangdese batholiths and Cretaceous ETB sources (detrital zircons with younger peaks < 300 Ma) as well from THS and HHC (detrital zircons with older peaks > 450 Ma) (Vadlamani et al. 2015). Furthermore, the detrital zircon age spectra from Bhuban

Formation of Surma Group of Assam foreland basin display major peaks centered around 550 Ma with younger peaks range between 27 and 123 Ma. The 550 Ma zircons were probably sourced from the THS with subordinate contributions from metamorphic rocks of the HHC and the LHS and the younger set of 27–123 Ma-aged zircons was due to the arc rocks of the Gangdese and ETB granitoids (Vadlamani et al. 2015). The U–Pb detrital zircon age data of Vadlamani et al. (2015) on the Barail and Surma sediments of AFB suggest the sediments were sourced from

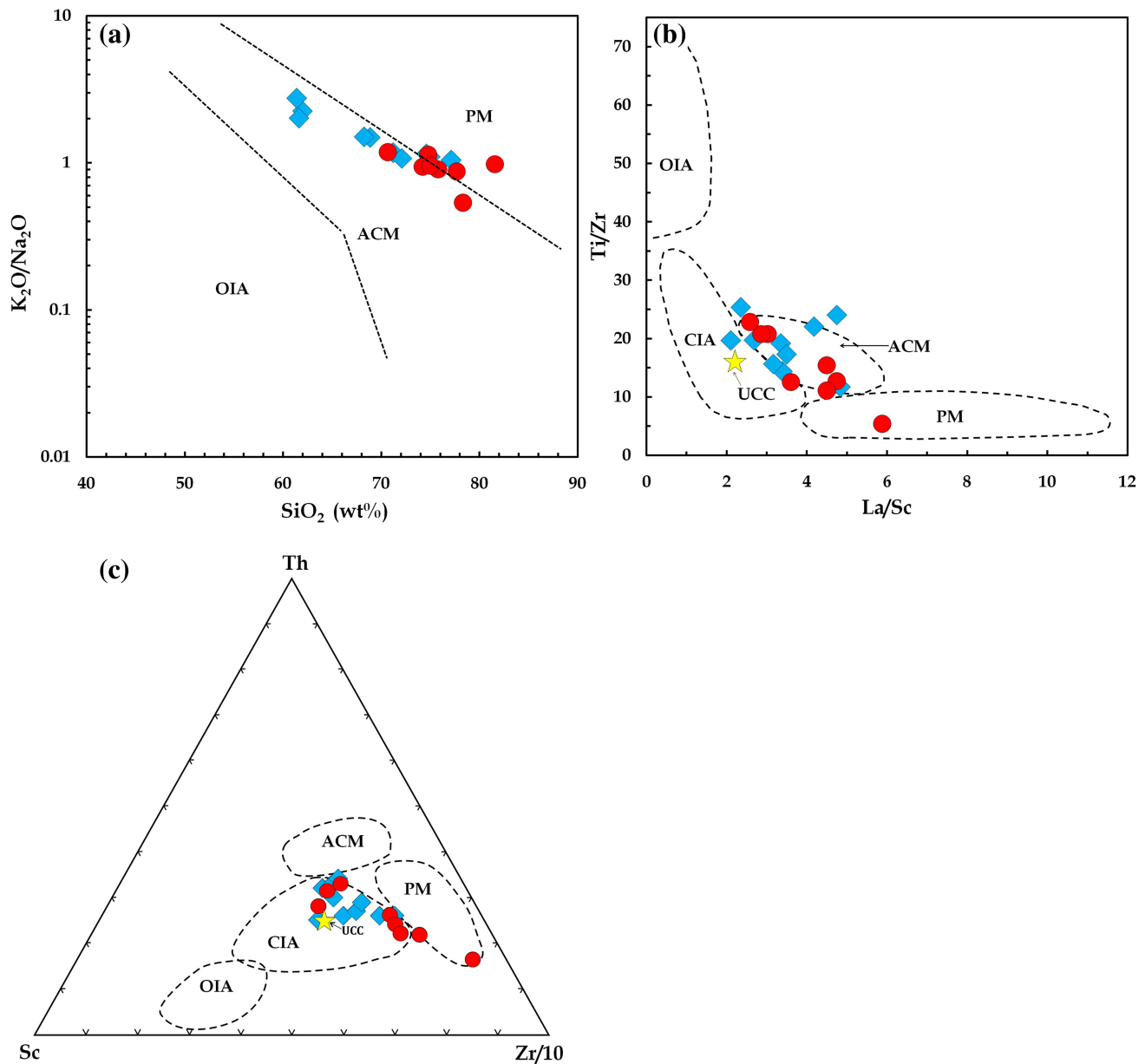


Fig. 12 Possible source rock and tectonic setting discrimination diagrams for Surma and Barail sediments from major and trace element ratios; OIA—oceanic island arc; CIA—continental island arc; ACM—active continental margin; PM—passive margin; discrimination fields in **a** after Roser and Korsch (1986) **b** and **c** after Bhatia and Crook (1986). The Upper Continental Crustal (UCC) values are after Taylor and McLennan (1985). Symbols are as in Fig. 5

eastern Trans-Himalayan granitoids/Gangdese batholiths and not from the Shillong plateau.

Shillong Plateau is comprised dominantly of ~ ca.1750–1600 Ma granitoid gneisses and ~ ca.500 Ma granitoids (Chatterjee et al. 2008; Yin et al. 2010; Chatterjee and Ghose 2011) of Pan-African affinity and lies to the east of MFB (Fig. 1a). Sawant et al. (2017) suggested the MFB sediments were derived from the Shillong plateau. In this context, the paleo course of the river Brahmaputra also appears crucial. In many previous studies including Uddin and Lundberg (1999), it was suggested that river Brahmaputra flowed from near the eastern Himalayan Syntaxis and apparently drained through the upper Assam valley and flowed through Mizoram Foreland Basin in the far east of the Shillong plateau and eventually drained to the Bay of Bengal (Fig. 11)

5.3 Tectonic settings

The tectonic setting for deposition of sedimentary strata is inferred based on the assumption that the nature of the source area is intimately related to the tectonic processes that control the origin and evolution of an adjacently lying sedimentary basin (Bhatia and Crook 1986). Variations in geochemical data on clastic sediments reflect distinct provenance types and associated tectonic settings for deposition of sedimentary sequences (Bhatia 1983; Bhatia and Crook 1986; Roser and Korsch 1986; Armstrong-Altrin and Verma 2005). In the SiO_2 versus $\text{K}_2\text{O}/\text{Na}_2\text{O}$ diagram of Roser and Korsch (1986) and Ti/Zr versus La/Sc diagrams of Bhatia and Crook (1986), the studied samples plot within the field for Active Continental Margin (ACM) settings (Fig. 12a, b). In the ternary $\text{Th-Sc-Zr}/10$ diagram of Bhatia and Crook (1986) all the samples plot within the field for Continental Island Arc settings except one Barail sample (SCZ 3) that plot within the field for Passive margin settings due to its very high Zr content (Fig. 12c). We therefore suggest that the sediments were deposited in an Active Continental Margin setting and were derived chiefly from the felsic lithounits of Himalaya.

6 Conclusions

The whole rock geochemical study of Tertiary Surma and Barail sandstones of Mizoram Foreland Basin was conducted to better constrain their source rock weathering, provenance, and tectonic settings. The results are summarized as:

1. Sandstones of the Barail and Surma Groups were classified as Quartzarenite and Sublithic-arenite based on the dominance of quartz and feldspar over a minor

presence of lithic clastics. Geochemical characteristics of the rock Groups were almost similar and plot in a singular array in various discrimination diagrams suggesting derivation of their precursor sediments from a singular source.

2. The weathering indices like CIA, CIW for the Barail and Surma sandstones suggest the precursor sediments were derived from a moderately weathered source.
3. In the A-CN-K diagram the Surma and Barail sandstones plotted along the regular weathering line originating from Granodioritic sources and were confined within the field for coeval Siwalik foreland sediments. Himalayan granitoids also plotted in the A-CN-K space close to the granodiorites. Integrating these, it appears that the sediments for the sandstones were probably derived from Himalayan granitoids.
4. Values of various trace element ratios including REE ratios and chondrite-normalized REE patterns for the Surma and Barail sandstones suggest a felsic magmatic source for both the Groups of rock.
5. On the basis of their plots in different tectonic discrimination diagrams it appears that the sediments were deposited in an active continental margin, and/or continental island arc tectonic settings sourced from Trans-Himalayan granitoids and Gangdese batholiths.

Acknowledgements Authors are thankful to the Director, Wadia Institute of Himalayan Geology, Dehradun, India for the analysis. BB thankfully acknowledges the financial support from UGC-NERO, Govt. of India [No. F.5-44/2013-14(MRP/NERO)/281] to carry out the work. We like to thank two anonymous reviewers for their critical reviews and suggestions and Dr. Binbin Wang (Managing Editor of the Journal) for the editorial handling and constructive suggestions which has enhanced the quality of the manuscript.

References

- Ahmad T, Harris NBW, Islam R, Khanna PP, Sachan HK, Mukherjee BK (2005) Contrasting mafic magmatism in the Shyok and Indus suture zones: geochemical constraints. *Him Geol* 26:33–40
- Allen R, Najman Y, Carter A, Barford D, Bickle MJ, Chapman HJ, Garzanti E, Vezzoli G, Ando S, Parrish RR (2008) Provenance of the Tertiary sedimentary rocks of the Indo-Burman Ranges, Burma (Myanmar): Burma arc or Himalayan derived? *J Geol Soc Lond* 165:1045–1057
- Andersson POD, Worden RH, Hodgson DM, Flint S (2004) Provenance evolution and chemostratigraphy of a Palaeozoic submarine fan-complex: Tanqua Karoo Basin, South Africa. *Mar Pet Geol* 21:555–577
- Armstrong-Altrin JS (2009) Provenance of sands from Cazones, Acapulco, and Bahía Kino beaches, Mexico. *Revista Mexicana de Ciencias Geológicas* 26(3):764–782
- Armstrong-Altrin JS, Verma SP (2005) Critical evaluation of six tectonic setting discrimination diagrams using geochemical data of Neogene sediments from known tectonic settings. *Sediment Geol* 177:115–129

- Armstrong-Altrin JS, Lee YI, Verma SP, Ramasamy S (2004) Geochemistry of sandstones from the Upper Miocene Kudankulam Formation, southern India: implications for provenance, weathering and tectonic setting. *J Sediment Res* 74(2):285–297
- Armstrong-Altrin JS, Nagarajan R, Madhavaraju J, Rosalez-Hoz L, Lee YI, Balaram V, Cruz-Martinez A, Avila-Ramirez G (2013) Geochemistry of the Jurassic and Upper Cretaceous shales from the Molango Region, Hidalgo, Eastern Mexico: implications of source-area weathering, provenance, and tectonic setting. *CR Geosci* 345:185–202
- Bhatia MR (1983) Plate tectonics and geochemical composition of sandstones. *Geol* 91:11–627
- Bhatia MR, Crook KAW (1986) Trace element characteristics of greywackes and tectonic setting discrimination of sedimentary basins. *Contrib Mineral Petrol* 92:181–193
- Bhuiyan MAH, Rahman MJ, Dampare SB, Suzuki S (2011) Provenance, tectonics and source weathering of modern fluvial sediments of the Brahmaputra-Jamuna River, Bangladesh: inference from geochemistry. *J Geochem Expl* 111:113–137
- Bock B, McLennan SM, Hanson GN (1998) Geochemistry and provenance of the middle Ordovician Austin glen member (Normanskill formation) and the Taconian Orogeny in new England. *J Sediment Res* 45:635–655
- Braccioli L, Marroni M, Pandolfi L, Rocchi S (2007) Geochemistry and petrography of Western Tethys Cretaceous sedimentary covers (Corsica and Northern Apennines): from source areas to configuration of margins. In: Arribas J, Critelli S, Johnsson MJ (eds) *Sedimentary provenance and petrogenesis: perspectives from petrography and geochemistry*. *Geol Soc Am Spec Pap* vol 420, pp 73–93
- Chatterjee N, Ghose NC (2011) Extensive early neoproterozoic high-grade metamorphism in North Chhotanagpur Gneissic Complex of the Central Indian Tectonic Zone. *Gond Res* 20:362–379
- Chatterjee N, Crowley JL, Ghose NC (2008) Geochronology of the 1.55 Ga Bengal anorthosite and Grenvillian metamorphism in the Chotanagpur Gneissic Complex, eastern India. *Precamb Res* 161:303–316
- Cina SE, Yin A, Grove M, Dubey CS, Shukla DP, Lovera OM, Kelty TK, Gehrels GE, Foster DA (2009) Gangdese arc detritus in the eastern Himalayan Neogene foreland basin: implications for the Neogene evolution of the Yarlung-Brahmaputra river system. *Earth Planet Sci Lett* 285:150–162
- Clift PD, Hodges KV, Heslop D, Hannigan R, Long HV, Claves G (2008) Correlation of Himalayan exhumation rates and Asian monsoon intensity. *Nat Geosci* 1:875–880
- Condie KC (1993) Chemical composition and evolution of upper continental crust: contrasting results from surface samples and shales. *Chem Geol* 104:1–37
- Cox R, Lowe DR, Cullers RL (1995) The influence of sediment recycling and basement composition on evolution of mudrock chemistry in the southwestern United States. *Geochim Cosmochim Acta* 59:2919–2940
- Cullers RL (1994a) The chemical signature of source rocks in size fractions of Holocene stream sediment derived from metamorphic rocks in the wet mountains region, Colorado, USA. *Chem Geol* 113:327–343
- Cullers RL (1994b) The controls on the major and trace element variation of shales, siltstones, and sandstones of Pennsylvanian-Permian age from uplifted continental blocks in Colorado to platform sediment in Kansas, USA. *Geochim Cosmochim Acta* 58:4955–4972
- Cullers RL (1995) The controls on the major and trace element evolution of shales, siltstones and sandstones of Ordovician to Tertiary age in the Wet Mountain region, Colorado, USA. *Chem Geol* 123:107–131
- Cullers RL (2000) The geochemistry of shales, siltstones and sandstones of Pennsylvanian-Permian age, Colorado, USA: implications for provenance and metamorphic studies. *Lithos* 51:181–203
- Cullers RL (2002) Implications of elemental concentrations for provenance, redox conditions and metamorphic studies of shales and limestones near Pueblo, Colorado, USA. *Chem Geol* 191:305–327
- Cullers RL, Podkopyrov VN (2002) The source and origin of terrigenous sedimentary rocks in the Mesoproterozoic Ural Group, southeastern Russia. *Precamb Res* 117:157–183
- Cullers RL, Barrett T, Carlson R, Robinson B (1987) Rare-earth element and mineralogic changes in Holocene soil and stream sediment: a case study in the Wet Mountains, Colorado, USA. *Chem Geol* 63:275–297
- Dasgupta S (1984) Tectonic trends in Surma basin and possible genesis of the folded belt. *Rec Geol Surv India* 113(IV):58–61
- Fedo CM, Nesbitt HW, Young GM (1995) Unraveling the effects of potassium metasomatism in sedimentary rocks and paleosols with implications for paleoweathering conditions and provenance. *Geology* 23:921–924
- Feng R, Kerrich R (1990) Geochemistry of fine-grained clastic sediments in the Archean Abitibi greenstone belt, Canada: implications for provenance and tectonic setting. *Geochim Cosmochim Acta* 54:1061–1081
- Floyd PA, Leveridge BE (1987) Tectonic environments of the Devonian Grams-Catho basin, south Cornwall: framework mode and geochemical evidence from turbidite sandstones. *J Geol Soc Lond* 144:531–542
- Floyd PA, Winchester JA, Park RG (1989) Geochemistry and tectonic setting of Lewisian clastic metasediments from the Early Proterozoic Loch Maree Group of Gairloch, N.W. Scotland. *Precamb Res* 45(1–3):203–214
- Gallet S, Jahn B, Van Vliet Lanoë B, Dia A, Rossello E (1998) Loess geochemistry and its implications for particle origin and composition of the upper continental crust. *Earth Planet Sci Lett* 156:157–172
- Galy A, France-Lanord C (2001) Higher erosion rates in the Himalaya: geochemical constraints on riverine fluxes. *Geology* 29:23–26
- Garcia D, Fonteilles M, Moutte J (1994) Sedimentary fractionations between Al, Ti, and Zr and the genesis of strongly peraluminous granites. *J Geol* 102:411–422
- Geological Survey of India (1974) Geology and mineral resources of the states of India, part IV—Arunachal Pradesh, Assam, Manipur, Meghalaya, Mizoram, Nagaland and Tripura. *Geol Surv India Misc Publ* 30:93–101
- Gu XX, Liu JM, Zheng MH, Tang JX, Qi L (2002) Provenance and tectonic setting of the proterozoic turbidites in Hunan, South China: geochemical evidence. *J Sediment Res* 72(3):393–407
- Harnois L (1988) The CIW index: a new chemical index of weathering. *Sediment Geol* 55:319–322
- Herron MM (1988) Geochemical classification of terrigenous sands and shales from core or log data. *J Sediment Petrol* 58:820–829
- Hossain HMZ, Roser BP, Kimura JI (2010) Petrography and whole-rock geochemistry of the Tertiary Sylhet succession, northeastern Bengal Basin, Bangladesh: Provenance and source area weathering. *Sediment Geol* 228:171–183
- Karunakaran C (1974) Geology and mineral resources of the north eastern states of India. *Geol Surv India Misc Publ* 30(4):93–101
- Karunakaran C, Ranga Rao A (1979) Status of exploration for hydrocarbons in the Himalayan region: contributions to stratigraphy and structure. *Geol Surv India Misc Publ* 41:1–66
- Ken-I Hayashi, Fujisawa H, Holland HD, Ohmoto H (1997) Geochemistry of 1.9 Ga sedimentary rocks from northeastern Labrador, Canada. *Geochim Cosmochim Acta* 61:4115–4137

- Konstantopoulos P, Zelilidis A (2012) Sedimentation of submarine fan deposits in the Pindos Foreland Basin, from Late Eocene to Early Oligocene, West Peloponnesus Peninsula, SW Greece. *Geol J* 48(4):335–362
- Madhavaraju J, Lee YI (2010) Influence of Deccan volcanism in the sedimentary rocks of Late Maastrichtian-Danian age of Cauvery basin Southeastern India: constraints from geochemistry. *Curr Sci* 98:528–537
- Malsawma J, Lalnuntluanga P, Badekar A, Sangode SJ, Tiwari RP (2010) Magnetic polarity stratigraphy of the Bhuban succession, Surma Group, Tripura-Mizoram accretionary belt. *J Geol Soc India* 76:119–133
- Mathur LP, Evans P (1964) Oil in India: special Brochure. In: Proceedings of the XXIIth international geological congress, New Delhi
- McLennan SM (1989) Rare earth elements in sedimentary rocks: influences of provenance and sedimentary processes. In: Lipin BR, McKay GA (eds) Geochemistry and mineralogy of rare earth elements, Mineral Soc America, vol 21, pp 169–200
- McLennan SM (2001) Relationships between the trace element composition of sedimentary rocks and upper continental crust. *Geochem Geophys Geosyst* 2:2000GC000109
- McLennan SM, Hemming S, McDaniel DK, Hanson GN (1993) Geochemical approaches to sedimentation, provenance and tectonics. *Geol Soc Am Spec Pap* 284:295–303
- Mitchell AHG, Htay MT, Htun KM, Win MN, Oo T, Hlaing T (2007) Rock relationships in the Mogok metamorphic belt, Tatkon to Mandalay, central Myanmar. *J Asian Earth Sci* 29:891–910
- Nagarajan R, Armstrong-Altrin JS, Nagendra R, Madhavaraju J, Moutte J (2007) Petrography and geochemistry of terrigenous sedimentary rocks in the Neoproterozoic Rabanpalli Formation, Bhima Basin, southern India: implications for paleoweathering condition, provenance and source rock composition. *J Geol Soc India* 70:297–312
- Najman Y (2006) The detrital record of orogenesis: a review of approaches and techniques used in the Himalayan sedimentary basins. *Earth Sci Rev* 74:1–72
- Najman Y, Bickle M, BouDagher-Fadel M, Carter A, Garzanti E, Paul M, Wijbrans J, Willett E, Oliver G, Parrish R, Akhter SH, Allen R, Ando S, Chisty E, Reisberg L, Vezzoli G (2008) The Paleogene record of Himalayan erosion: Bengal Basin, Bangladesh. *Earth Planet Sci Lett* 273:1–14
- Nandy DR (2001) Geodynamics of Northeastern India and the adjoining region. ACB Publication, Kolkata, p 209
- Nesbitt HW, Young GM (1982) Early Proterozoic climates and plate motions inferred from major element chemistry of lutites. *Nature* 299:715–717
- Nesbitt HW, Young GM (1984) Prediction of some weathering trends of plutonic and volcanic rocks based on thermodynamic and kinetic considerations. *Geochim Cosmochim Acta* 48:1523–1534
- O'Brien PJ (2001) Subduction followed by collision: Alpine and Himalayan examples. *Phys Earth Planet Inter* 127:277–291
- Parker A (1970) An index of weathering for silicate rocks. *Geol Mag* 107:501–504
- Pettijohn FJ, Potter PE, Siever R (1972) Sand and sandstones. Springer, New York
- Rahman MJJ, Suzuki S (2007) Geochemistry of sandstones from the Miocene Surma Group, Bengal Basin, Bangladesh: implications for provenance, tectonic setting and weathering. *Geochem J* 41:415–428
- Rahman MJJ, Sayem ASM, McCann T (2014) Geochemistry and provenance of the Miocene sandstones of the Surma Group from the Sitapahar Anticline, Southeastern Bengal Basin, Bangladesh. *J Geol Soc India* 83:447–456
- Rahman MJJ, Xiao W, McCann T, Songjian A (2017) Provenance of the Neogene Surma Group from the Chittagong Tripura Fold Belt, Southeast Bengal Basin, Bangladesh: constraints from whole-rock geochemistry and detrital zircon U–Pb ages. *J Asian Earth Sci* 148:277–293
- Ralte VZ, Tiwari RP, Lalchawimawii Malsawma J (2011) Selachian fishes from Bhuban Formation, Surma Group, Aizawl, Mizoram. *J Geol Soc India* 77:328–348
- Ramachandran A, Madhavaraju J, Ramasamy S, Lee YI, Rao S, Chawngthu DL, Velmurugan K (2016) Geochemistry of the Proterozoic clastic rocks of Kerur Formation of Kaladgi-Badami Basin, northern Karnataka, south India: implications for paleoweathering and provenance. *Turk J Earth Sci* 25:126–144
- Ranjan N, Banerjee DM (2009) Central Himalayan crystallines as the primary source for the sandstone-mudstone suites of the Siwalik Group: new geochemical evidence. *Gondwana Res* 16:687–696
- Rao DR, Rai H (2006) Signatures of rift environment in the production of garnet-amphibolites and eclogites from Tso-Morari region, Ladakh, India: a geochemical study. *Gondwana Res* 9:512–523
- Raza M, Ahmad AHM, Khan MS, Khan F (2012a) Geochemistry and detrital modes of Proterozoic sedimentary rocks, Bayana Basin, north Delhi fold belt: implications for provenance and source-area weathering. *Int Geol Rev* 54(1):111–129
- Raza M, Khan A, Bhardwaj VR, Rais S (2012b) Geochemistry of Mesoproterozoic sedimentary rocks of upper Vindhyan Group, southeastern Rajasthan and implications for weathering history, composition and tectonic setting of continental crust in the northern part of Indian shield. *J Asian Earth Sci* 48:160–172
- Reimann K-U (1993) Geology of Bangladesh. Gebruder Borntraeger, Berlin
- Robinson RAJ, Brezina CA, Parrish RR, Horstwood MSA, Oo NW, Bird MI, Thein M, Walters AS, Oliver GJH, Zaw K (2014) Large rivers and orogens: the evolution of the Yarlung Tsangpo-Irrawaddy system and the eastern Himalayan syntaxis. *Gond Res* 26:112–121
- Roddaz M, Viers J, Brusset S, Baby P, Boucayrand C, Heral G (2006) Controls on weathering and provenance in the Amazonian foreland basin: insights from major and trace element geochemistry of Neogene Amazonian sediments. *Chem Geol* 226:31–65
- Roser BP, Korsch RJ (1986) Determination of tectonic setting of sandstone–mudstone suites using SiO_2 content and $\text{K}_2\text{O}/\text{Na}_2\text{O}$ ratio. *J Geol* 94:635–650
- Roser BP, Korsch RJ (1999) Geochemical characterization, evolution and source of a Mesozoic accretionary wedge: the Torlesse terrane, New Zealand. *Geol Mag* 136:493–512
- Roy DK, Roser BP (2013) Geochemical evolution of the Tertiary succession of the NW shelf, Bengal basin, Bangladesh: implications for provenance, paleoweathering and Himalayan erosion. *J Asian Earth Sci* 78:248–262
- Saini NK, Mukherjee PK, Rathi MS, Khanna PP (2000) Evaluation of energy dispersive X-ray fluorescence spectrometry in the analysis of silicate rocks using pressed powder pellets. *X-ray Spectrom* 29:166–172
- Sawant SS, Kumar KV, Balaram V, Subba Rao DV, Rao KS, Tiwari RP (2017) Geochemistry and genesis of Craton-derived sediments from active continental margins: insights from the Mizoram Foreland Basin, NE India. *Chem Geol* 470:13–32
- Sharma R, Gupta V, Arora BR, Sen K (2011) Petrophysical properties of the Himalayan granitoids: implication on composition and source. *Tectonophysics* 497:23–33
- Sinha RN, Sastri VV (1973) Correlation of the Tertiary geosynclinal sediments of the Surma valley, Assam and Tripura state (India). *Sediment Geol* 10:107–134

- Sun L, Gui H, Chen S (2012) Geochemistry of sandstones from the Neoproterozoic Shijia Formation, northern Anhui Province, China: implications for provenance, weathering and tectonic setting. *Chemie der Erde-Geochem* 72:253–260
- Taylor SR (1965) The application of trace-element data to problems in petrology. In: Ahrens LH, Press F, Runcorn SK, Urey HC (eds) Physics and chemistry of the Earth 6. Pergamon, Oxford, pp 133–213
- Taylor SR (1969) Trace element chemistry of andesites and associated calc-alkaline rocks. In: McBirney AR (ed) Proceedings of the andesite conference. Department of Geology and Mineral Industries, Oregon, pp 43–63
- Taylor SR, McLennan SM (1985) The continental crust: its composition and evolution. Blackwell, London
- Tijani MN, Nton ME, Kitagawa R (2010) Textural and geochemical characteristics of the Ajali Sandstone, Anambra Basin, SE Nigeria: implication for its provenance. *Comptes Rendus Geosci* 342:136–150
- Tiwari RP, Mehrotra RC (2002) Plant impressions from the Barail Group of Champhai-Aizawl road section, Mizoram, India. *Phytomorphology* 52:69–76
- Tiwari RP, Sangode SJ, Patil SK, Sivaji Ch, Arora BR (2006) Status of palaeomagnetic and magnetostratigraphic studies in the North East India and the new initiatives. *Deep Cont Stud India Newslett* 16:16–20
- Uddin A, Lundberg N (1998) Cenozoic history of the Himalayan-Bengal system: sand composition in the Bengal basin, Bangladesh. *Geol Soc Am Bull* 110:497–511
- Uddin A, Lundberg N (1999) A paleo-Brahmaputra? Subsurface lithofacies analysis of Miocene deltaic sediments in the Himalayan-Bengal system, Bangladesh. *Sediment Geol* 123:239–254
- Vadlamani R, Wu F-Y, Ji W-Q (2015) Detrital zircon U-Pb age and Hf isotopic composition from foreland sediments of the Assam Basin, NE India: constraints on sediment provenance and tectonics of the Eastern Himalaya. *J Asian Earth Sci* 111:254–267
- Wang W, Zhou MF (2013) Petrological and geochemical constraints on provenance, paleoweathering, and tectonic setting of the Neoproterozoic sedimentary basin in the eastern Jiangnan Orogen, South China. *J Sed Res* 83:975–994
- Wang W, Zhou MF, Yan DP, Li JW (2012) Depositional age, provenance, and tectonic setting of the Neoproterozoic Sibao Group, southeastern Yangtze Block, South China. *Precamb Res* 192–195:107–124
- Webb AAG, Yin A, Harrison TM, Célérier J, Gehrels GE, Manning CE, Grove M (2011) Cenozoic tectonic history of the Himachal Himalaya (northwestern India) and its constraints on the formation mechanism of the Himalayan orogen. *Geosphere* 7(4):1013–1061
- Yin A, Dubey CS, Webb AAG, Kelty TK, Grove M, Gehrels GE, Burgess WP (2010) Geological correlation of the Himalayan orogen and Indian craton. Part 1. Structural geology, U-Pb zircon geochronology, and tectonic evolution of the Shillong Plateau and its neighbouring regions in NE India. *Geol Soc Am Bull* 122:336–359
- Young GM, Nesbitt HW (1998) Process controlling the distribution of Ti and Al in weathering profiles, siliciclastic sediments and sedimentary rocks. *Sediment Res* 68:448–455